



Solid-State NMR on Complex Biomolecules: **23** Methods and Applications

Deni Mance, Markus Weingarth, and Marc Baldus

Contents

Introduction	488
Methods	488
ssNMR Sample Preparation for Complex Biomolecules	488
Solid-State NMR Methodology for Complex Systems	491
Applications	494
Fibrils and Other Protein Assemblies	494
Biomaterials	496
Conclusions	499
References	500

Abstract

Solid-state NMR (ssNMR) can provide structural information at the most detailed level and, at the same time, is applicable in highly heterogeneous and complex molecular environments, largely irrespective of solubility or crystallinity. In the following chapter, we discuss concepts to deal with the spectroscopic challenges of applying ssNMR to complex biomolecular systems and how to place structural information obtained from ssNMR in a (supra)molecular context. Applications range from protein biopolymers and hydrogels to drug delivery systems, biosilica, and other biomaterials.

Keywords

Solid-state NMR · Drug delivery systems · Cells · Amyloids · DNP · Hydrogels · Biosilica · MD simulations · Coarse-grained simulations · Humins · Microtubules

D. Mance · M. Weingarth · M. Baldus (✉)
NMR Spectroscopy, Bijvoet Center for Biomolecular Research, Utrecht University, Utrecht, CH,
The Netherlands
e-mail: m.baldus@uu.nl

Introduction

Solid-state NMR (ssNMR) belongs to a small number of experimental methods that can provide structural information at the most detailed level and, at the same time, is applicable in highly heterogeneous and complex molecular environments largely irrespective of solubility or crystallinity [1]. The main challenge associated with the use of ssNMR in complex molecular systems refers to the ability to detect the molecule of interest with adequate spectroscopic resolution and sensitivity. In the last years, significant progress has been made in addressing both issues by advancements in the field of ssNMR instrumentation and sample preparation as well as by implementing novel pulse sequences and data acquisition schemes. At the same time, developments in related fields such as electron and light microscopy as well as in computational structural biology and theoretical chemistry have provided novel opportunities to obtain a comprehensive, ssNMR-based view of the supramolecular arrangement of complex molecular systems in both life and material science applications.

In the following chapter, we will discuss concepts to deal with the spectroscopic challenges of ssNMR applied to complex biomolecular systems and how to place structural information obtained from ssNMR in a (supra)molecular context. We will give examples on how these approaches can be used to study complex biomolecular systems ranging from amyloid proteins to drug delivery systems and biosilica. As an example of the growing opportunities for *in situ* studies of ssNMR, we will highlight preparative advancements in the field of cellular solid-state NMR to study functional cell organelles such as bacterial cell envelopes and eukaryotic plasma membrane vesicles. The interested reader is referred to additional studies of our group in which ssNMR has been used in the context of membrane proteins and their complexes [2] as well as in material science applications including catalyst materials [3] and colloidal nanocrystals [4].

Methods

ssNMR Sample Preparation for Complex Biomolecules

Solid-state NMR provides increasing possibilities to study complex molecular systems under “*in situ*” conditions. In the case of biomolecules, tailored isotope-labeling approaches for pro- and eukaryotic systems are usually required. Virtually all NMR studies conducted today on proteins or other biomolecules use isotope labeling to enhance NMR signals and to allow for multidimensional ssNMR correlation spectroscopy.

However, with increasing size and molecular complexity, isotope labeling and protein overexpression may not be sufficient to detect ssNMR signals of a particular protein in its natural biological environment. An example of such a situation refers to the outer membrane of Gram-negative bacteria where endogenous protein expression levels of naturally highly abundant outer membrane proteins, *i.e.*, OmpA and OmpF, may be comparable to the membrane protein of interest, even under the

conditions of overexpression. In this case, studies using cellular envelopes or whole cells of Gram-negative bacteria are facilitated by the use of an *E. coli* deletion strain to remove signals from naturally highly abundant outer MPs [5, 6]. In such preparations, signals from other cellular components including lipids, nucleotides, peptidoglycan, and lipopolysaccharides remain visible at intensities similar to the (overexpressed) protein of interest. Another strategy to minimize background labeling refers and relates to adding rifampicin to the growth medium in order to specifically label the target protein of interest by inhibiting expression of endogenous proteins [5, 6]. Obviously, non-proteinaceous cell components such as nucleotides and lipids remain labeled. To further suppress such contributions, specific editing methods such as discussed in Refs. [5, 7] can be used.

Escherichia coli is a well-established host for protein expression using minimal media. However, high-quality functional expression of proteins from higher organisms often requires a eukaryotic host system to ensure proper protein folding, posttranslational modification, and membrane insertion. A way to circumvent the problem of protein production in higher organisms and still achieve posttranslational modifications concerns the use of specific enzymes during the protein production for NMR purposes. For example, the *O*-GlcNAc transferase (OGT) transfers GlcNAc moieties from UDP-GlcNAc to serines and threonines of numerous target proteins, including those produced in *E. coli*. We utilized the latter aspect to produce ^{13}C , ^{15}N -labeled nucleoporins (Nups) that are natively heavily modified by *O*-linked β -*N*-acetylglucosamines [8]. In addition, significant progress has been made in the last years to express and purify proteins from eukaryotic cells. Fully and specifically ^{13}C , ^{15}N -labeled proteins suitable for NMR studies were produced from different eukaryotic cell types (see, e.g., Ref. [2] for a recent review). Yet, the costs for producing such samples can still be prohibitive.

In our laboratory, we [9] could recently produce fully and specifically labeled membrane vesicles derived from A431 cells (human cancer cells), which are known to express high levels of the epidermal growth factor receptor (EGFR) allowing us to perform ssNMR studies on functional EGF receptors in the natural membrane environment. For isotope labeling, we adapted published procedures using a combination of dialyzed fetal calf serum and labeled amino acid mixtures obtained from algae extracts to produce a ^{13}C , ^{15}N -enriched medium. While NMR has been readily used to study soluble proteins associated with entire bacterial or eukaryotic cells (see, e.g., [10]), producing specific organelles offers a means to study molecular components such as membrane proteins in their native cell environment at enhanced spectroscopy sensitivity. For example, we produced [9] plasma membrane vesicles from lysed A431 cells that contain an increased level of functional receptor and, at the same time, reflect vesicles that are about an order of magnitude smaller than eukaryotic cells (Fig. 1), thereby enhancing signal to noise for ssNMR studies significantly.

Finally, novel preparative and labeling routes are also needed for proton-detected ssNMR experiments in complex biomolecular systems. ^1H -detection in solid-state NMR can much improve spectral sensitivity and resolution. However, ^1H -detection has thus far much relied on perdeuteration, which prevents detection of nonexchangeable

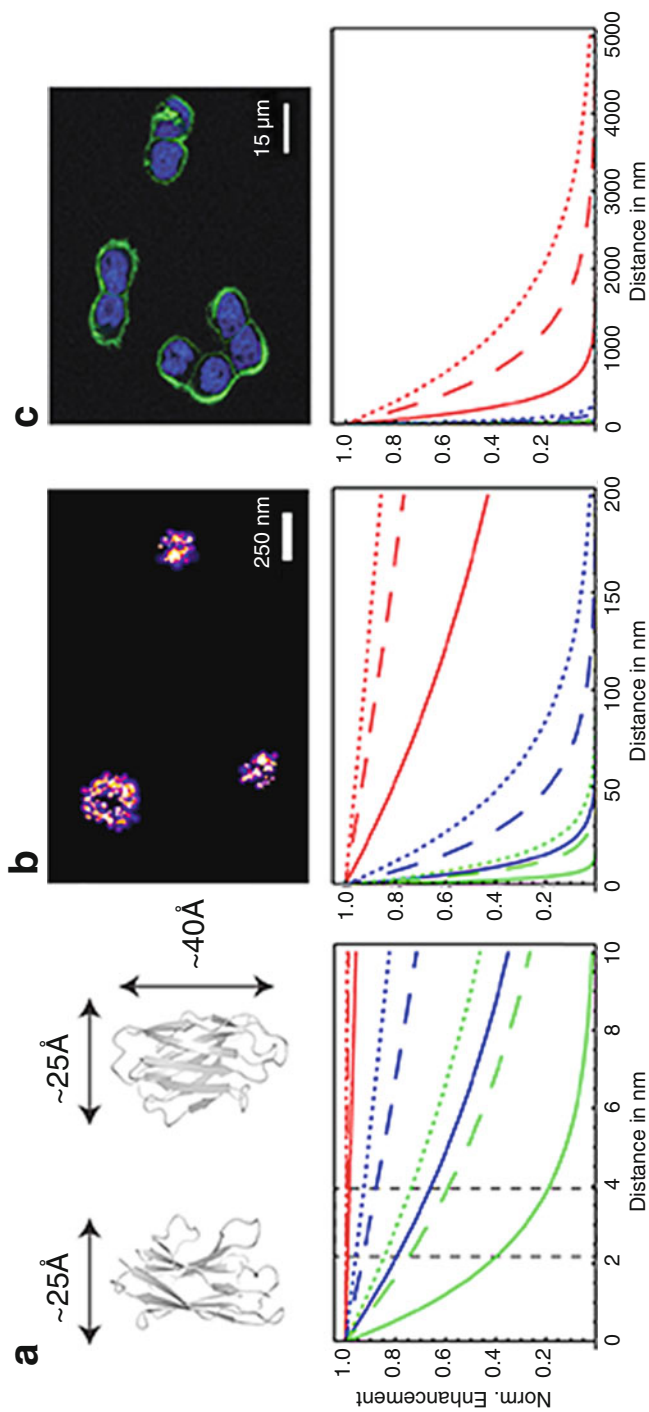


Fig. 1 Model calculations assuming an initial creation of DNP-enhanced magnetic polarization that is transferred to the interior of molecules of different size via spin diffusion. In each case, polarization was computed for the indicated distance from the molecular surface for average ^1H - ^1H distances of 1 Å (red), 5 Å (blue), and 10 Å (green). In addition, we varied $T_{1\text{in}}$ relaxation times from 1 s (solid lines), 10s (dashed lines), and 30 s (dotted lines)

protons such as side-chain protons. To overcome this limitation, we have recently introduced several approaches that make nonexchangeable protons amenable to ^1H -detection at high spectral resolution (vide infra, section “ [\$^1\text{H}\$ -Detection](#)”).

Solid-State NMR Methodology for Complex Systems

Dynamic Nuclear Polarization (DNP)

A critical parameter for studying complex molecular systems refers to spectroscopic sensitivity. This challenge has been addressed in the field of ssNMR by the advent of commercial DNP (dynamic nuclear polarization, Ref. [11]) NMR instruments that currently can operate at 400 MHz, 600 MHz, and up to 800 MHz NMR frequency. High-field conditions [12] are particularly attractive for complex molecular systems including membrane proteins [6, 9, 13] or intact biomaterials [14, 15]. Yet, recent work has shown that DNP enhancements can significantly vary and generally reduce with increasing magnetic field in the case of biradicals that utilize the cross effect [2]. Mance et al. have recently examined [16] the magnetic field dependence of biradicals including AMUPol [17]. These studies suggested an approximately $1/B_0^2$ dependence of cross-effect DNP that is governed by a relative weak effective hyperfine coupling that describes the initial electron-nuclear polarization transfer step. The corresponding distance amounts to approximately 10 Å which is line with experimentally observed paramagnetic relaxation enhancement (PRE) effects under low-temperature DNP conditions [12, 18]. Since the polarization in DNP is usually distributed by spin-diffusion processes among protons, this observation suggests that core protons near the biradical act as a “polarization sink” since they do not contribute in the spin-diffusion process but could still get polarized. Recently, this effect has been observed experimentally [19] using various deuterated biradicals, where after deuteration of the core protons, a beneficial effect on the DNP enhancement was detected. Moreover, recent studies [20] as well as ongoing work in our laboratory suggest that trityl-based biradicals may be better suited for ultrahigh-field DNP studies in the future.

Next to sensitivity, spectroscopic resolution is another critical factor for DNP applications on complex (bio)molecules. This parameter was recently examined by comparing two-dimensional (^{13}C , ^{13}C) and (^{15}N , ^{13}C) correlation data sets on fully ^{13}C , ^{15}N -labeled variants of the KcsA potassium channel at 800 MHz DNP conditions using soluble [12] and tagged [18] AMUPol variants to data obtained at ambient temperatures. In line with previous low-temperature ssNMR studies work on unfolded [21] proteins, it was found that local protein motion represents an important factor in determining the experimentally observed line width under LT-DNP conditions [22].

Because the resulting DNP signal enhancement is dictated by spin-diffusion processes, the relative DNP enhancement of locally separated molecular subsystems can report on supramolecular structure. For example, in the case of biosilica (see section “[Biosilica](#)”), which consists of different molecular layers, i.e., polysaccharides, peptides, polyamines, and silica, the DNP biradical will be confined to the

surface. As a result, polarization created from water-soluble biradicals will be spread to the inner molecular layers by spin diffusion that can be treated classically using Fick's law. In this formalism, the longitudinal nuclear relaxation time (T_{1n}) and the diffusion constant (which depends on the average ^1H - ^1H distance) will ultimately determine the local DNP enhancement. Since biosilica consist of different molecular layers (determined by specific diffusion constants and T_{1n} parameters), theoretical models can be compared to the measured enhancements to estimate the thickness of each layer (see section "**Biosilica**" and Ref. [15]).

Such considerations can also be extended to predict the effect of variations in proton density on the resulting DNP enhancement for a wide range of molecular sizes. In Fig. 1a, a small protein with a dimension of approximately 5 nm dimension is compared to plasma membrane vesicles [9] (about 200 nm's, Fig. 1b) and entire eukaryotic cells (Fig. 1c, 15 μm). As visible in Fig. 1 (lower panel), DNP enhancements are largely constant in small proteins, unless high levels of proton dilution (such as fractional deuteration or perdeuteration; see section " **^1H -Detection**") are used and, at the same time, short T_{1n} relaxation times are active. This situation significantly changes in the case of plasma membrane vesicles where only full protonation allows for relatively constant DNP enhancement factors across each vesicle. Finally, sizable DNP enhancements are largely confined to approximately a micrometer ring on the outside of mammalian cells when soluble DNP radicals are added. In summary, a nonuniform distribution of the polarization can be created by using larger molecular dimensions or by chemically modulating spin-diffusion as well as relaxation parameters.

^1H -Detection

Another means to enhance spectral sensitivity in solid-state NMR is by detecting protons. Spectral sensitivity is proportional to $\gamma^{3/2}$, i.e., the detection of ^1H instead of ^{15}N can potentially increase spectral sensitivity by a factor of ~ 30 . Yet, while ^1H has been the detection nuclei of choice in biological solution NMR ever since, ^1H -detection in biological solids has been prevented by the presence of strong and time-dependent homonuclear proton couplings that largely broaden the ^1H linewidth. Fortunately, the advents of fast (>50 kHz) MAS probeheads and dilution of the proton network with perdeuteration labeling have provided the tools to detect protons in the solid state. This is a big advantage for biological solid-state NMR studies. Next to gains in sensitivity, which enable the use of submicrogram quantities of labeled proteins, ^1H -detection also adds another spectral dimension to the usual ^{13}C and ^{15}N dimensions and thereby improves spectral resolution. The perdeuteration approach has been successfully applied to globular proteins and amyloid fibrils as well as water-exposed regions of membrane proteins (see, e.g., Refs. [23–26]).

However, perdeuteration, based on protein expression in fully deuterated media, only allows access to exchangeable amino protons. This prevents ^1H -detection of side-chain ^1H , which is crucial for structure determination, as well as access to water-inaccessible protein regions such as the transmembrane domains (TMs) of membrane proteins. Weingarth et al. have recently introduced three labeling schemes

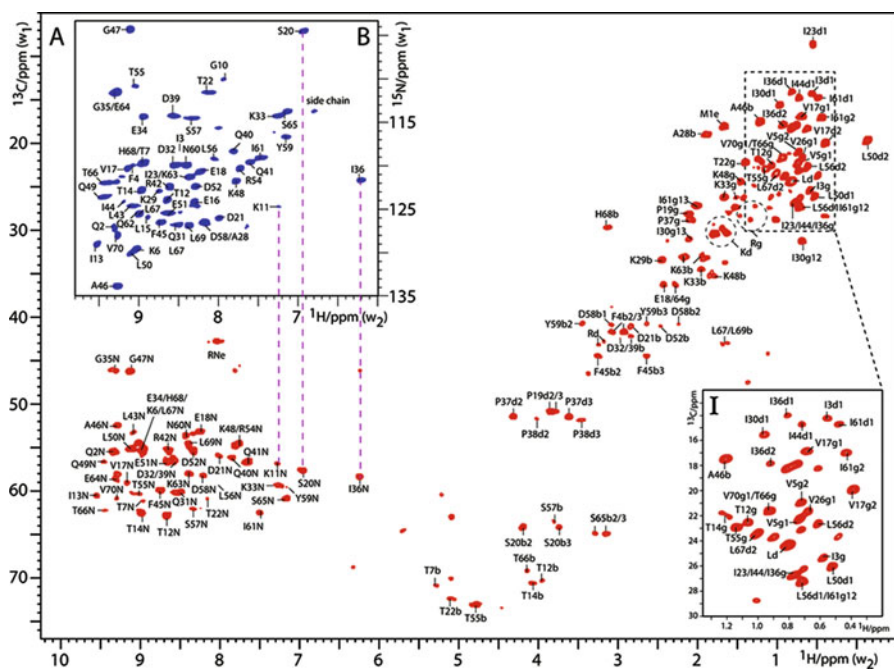


Fig. 2 ^1H -detected solid-state NMR experiments in fractionally deuterated ubiquitin. This labeling scheme provides a very good ^1H -resolution well below 0.1 ppm for both (a) exchangeable amino protons and the (b) nonexchangeable side-chain protons (Adapted from Ref. [28])

that overcome these problems: (1) ^1H -cloud labeling, which incorporates fully protonated types of amino acids (referred to as “ ^1H -clouds”) in a perdeuterated protein matrix [27]. This strategy provides well-resolved aliphatic side-chain ^1H resonances and enables the measurement of inter-residual proton-proton contacts between ^1H side chains, which was demonstrated in ubiquitin and in beta-barrel membrane protein BamA. (2) Another approach refers to fractional deuteration, which is based on protein growth in D_2O (100%) and fully protonated glucose [28]. This labeling scheme yields labeled proteins that feature many carbons, such as the alpha-carbons, that are virtually devoid of protons, while other carbons retain a sizable proton density. This labeling scheme allows both assigning side-chain ^1H and harnessing side-chain ^1H for structural studies, which was demonstrated in ubiquitin and applied to the K^+ channel KcsA (Fig. 2). Moreover, this labeling scheme allows for the direct detection of functionally important structural water molecules [28]. (3) In addition, Weingarth et al. introduced another labeling scheme, named inverse fractional deuteration (iFD, Ref. [29]), which is based on using H_2O in the growth medium and hence allows for the detection of water-inaccessible proteins, even in situ. This labeling strategy was successfully used to study the slow ^{15}N $T_{1\rho}$ dynamics of the water-inaccessible selectivity filter of a membrane-embedded K^+ channel.

Furthermore and for the first time ever, protein detection could be used to obtain a high-resolution spectrum of a membrane protein in a native bacterial cell membrane.

Finally, ^1H -detection using fully protonated proteins also provides the potential to measure water-inaccessible proteins, such as in a membrane protein [30]. This approach bears even more potential for applications using MAS frequencies above 100 kHz where spectral resolution is further improved [31].

Combining ssNMR and Computational Approaches

Integrating solid-state NMR data with computational methods offers very attractive means to improve the structural interpretation of NMR data. While this approach has long been employed for 3D structure determination in NMR, it also allows translating relaxation rates in motional modes, chemical shifts in structural data, or water exposure into molecular topology. For example, the water exposure of biomolecules, as measured by T_2 -edited 2D H(H)C experiments, can be quantitatively back-calculated over long atomistic molecular dynamics (MD) simulations, which allows probing peptide topology and insertion depth in a membrane setting [32].

A particularly interesting approach is the integration of solid-state NMR with mesoscopic coarse-grained simulations, which can, for example, be performed with the MARTINI force field [33]. Such force fields allow for computations of large systems (millions of beads) over large timescales (microsecond to milliseconds). It was shown that these simulations, in combination with solid-state NMR data, allow probing peptide assembling [34], membrane remodeling [14], and specific lipid binding to membrane proteins [35]. Van der Crujisen et al. also demonstrated on the example of K^+ channels that specific lipid binding predicted by atomistic MD simulations can be experimentally validated with frequency-selectivity solid-state NMR experiments [36]. Finally, the analysis of solid-state NMR spectra can also be simplified via computational programs such as FANDAS [37], which provides a convenient means to predict multidimensional NMR spectra, thereby supporting spectral assignments.

Applications

The use of ssNMR-based concepts discussed in section “[Methods](#)” for studies on membrane proteins, their complexes, and cellular preparations has already been discussed in the literature [2, 38]. In the following, examples are given for applications to protein assemblies and a variety of biomaterials and drug delivery systems.

Fibrils and Other Protein Assemblies

Solid-state NMR has become the leading method to obtain structural and dynamics information on amyloid fibrils [39] including those formed by α -synuclein [40], tau [41, 42], and polyglutamine [43] (Fig. 3a, lower panel). Combining dipolar and scalar-based experiments (see, e.g., Ref. [40]) allows to identify core fibril residues

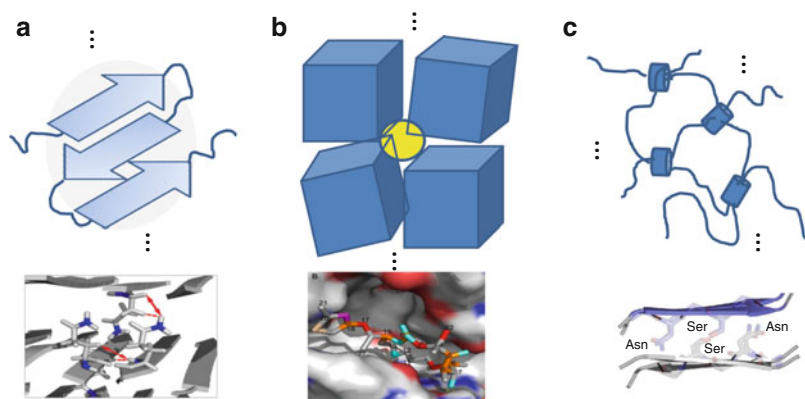


Fig. 3 (a) Solid-state NMR has become the leading method to obtain structural and dynamics information on amyloid fibrils such as polyglutamine fibrils where ssNMR provided insight into the side-chain packing (*lower panel*, adapted from [43]). In addition, it can be used to study ligand binding such as epothilone B (*lower panel*) to microtubules (**b**, adapted from Ref. [46]). Finally, ssNMR also provides a unique tool to study networking in protein hydrogels such as those obtained for proteins of the nuclear pore complex (**c**) (*Lower panel* adapted from Ref. [49])

and dynamic, surface-exposed segments, respectively. In the case of α -synuclein, it was also observed that β -strand regions identified from ssNMR in fibrils may already form transiently in protein monomers [44].

While a structural hallmark of amyloid fibrils is the beta-strand-rich fold, protein can also oligomerize or polymerize in other folds. For example, ssNMR data previously showed that protein needles formed *in vitro* by the type III secretion system protein undergo a conformational change upon needle formation [45] that leaves large portions of the monomer structure intact. Another example of protein polymerization refers to the polymerization of $\alpha\beta$ -tubulin into microtubules (MTs). MTs exist in a dynamic equilibrium with the nonpolymerized form, tubulin, a heterodimeric protein consisting of one α -tubulin subunit and one β -tubulin subunit. The dynamic behavior of MTs plays a crucial role in cell division making MTs an important target for anticancer drug design. It was previously shown [46] that ssNMR can be a powerful tool to study ligand binding to MTs (Fig. 3b). In particular, Kumar et al. compared 2D ssNMR data on free isotope-labeled epothilone B (Epo B) which belongs to a new class of anticancer compounds from the *myxobacterium Sorangium cellulosum* to data obtained after binding to MTs. Significant chemical shift changes were observed providing insight into possible binding modes of Epo B to MTs (Fig. 3b, lower panel). This study and work from Polenova et al. [47] underlines the potential of ssNMR to obtain information about binding to MTs by ssNMR.

Finally, there is an increasing number of protein-rich assemblies that contain intrinsically disordered protein domains and yet can form stable molecular networks *in vitro* and *in vivo*. In the latter case, such molecular assemblies have been termed signalosomes, granules, foci, or puncta which have recently received significant

attention [48]. Using proteins related to the nuclear pore complex that form hydrogels under *in vitro* conditions, we could previously demonstrate the power of ssNMR to study structural organization and dynamics of such assemblies, namely, of so-called NUPs comprising several hundred amino acids [8, 49]. In particular, it was shown for the case of the 62 kDa FG repeat domain of the nucleoporin Nsp1p that transient hydrophobic interactions between Phe and methyl side chains and intermolecular beta-sheets between the Asn-rich spacer regions (Fig. 3c, lower panel) are responsible for stabilization of the hydrogel. The data, therefore, suggested a fully unexpected cellular function of such interchain β -structures in maintaining the permeability barrier of nuclear pores.

Biomaterials

Lipid-Anchored Peptides

The phenomenon of protein aggregation in amyloid proteins also triggered the development of novel pharmaceutical and hybrid biomaterials, including lipid-anchored peptides, that may potentially be of pharmacological use in the context of immunotherapy-based approaches against neurodegenerative disorders such as Alzheimer's disease. Such preparations usually exhibit low peptide concentrations, and isotope labeling for NMR studies is costly. For these reasons, dynamic nuclear polarization NMR spectroscopy can provide an efficient means to obtain structural information on liposomal vaccines targeting Alzheimer's disease. Indeed, it was shown [14] that 2D double-quantum-filtered (2Q/1Q) ^{13}C correlation spectroscopy provides under DNP conditions (Fig. 4a) a powerful means to infer the structural organization of (N-terminal, selectively isotope-labeled) A β peptides in different lipid formulations. In particular, we found that DMPC/DMPG/cholesterol mainly stabilizes extended structures of the lipid-anchored peptide (Fig. 4b), while in DMTAP/cholesterol liposomes, the peptide adopts a multitude of conformations including random-coil and extended structures. In this study, we also successfully combined scarce ssNMR data (i.e., secondary chemical shifts) with mesoscopic coarse-grained molecular dynamics (CGMD) simulations to obtain a model of peptide association in vesicles.

Biosilica

Diatom biosilica is an inorganic/organic hybrid with interesting properties. The molecular architecture of the organic material at the atomic and nanometer scale has so far remained unknown, in particular for intact biosilica. The combination of DNP experiments with microscopy, mass spectrometry (MS), and molecular dynamics (MD) simulations recently [15] provided insight into the structural characterization of such systems. In line with our discussion in section “[Dynamic Nuclear Polarization \(DNP\)](#),” DNP resulted in the selective enhancement of protein backbone nitrogen signals at 120 ppm in the ^{15}N direct excitation (DE) MAS NMR spectra. In contrast, signals from LCPAs or lysine side chains remained absent even in the DNP-enhanced ^{15}N DE MAS NMR spectrum and were only detectable in the

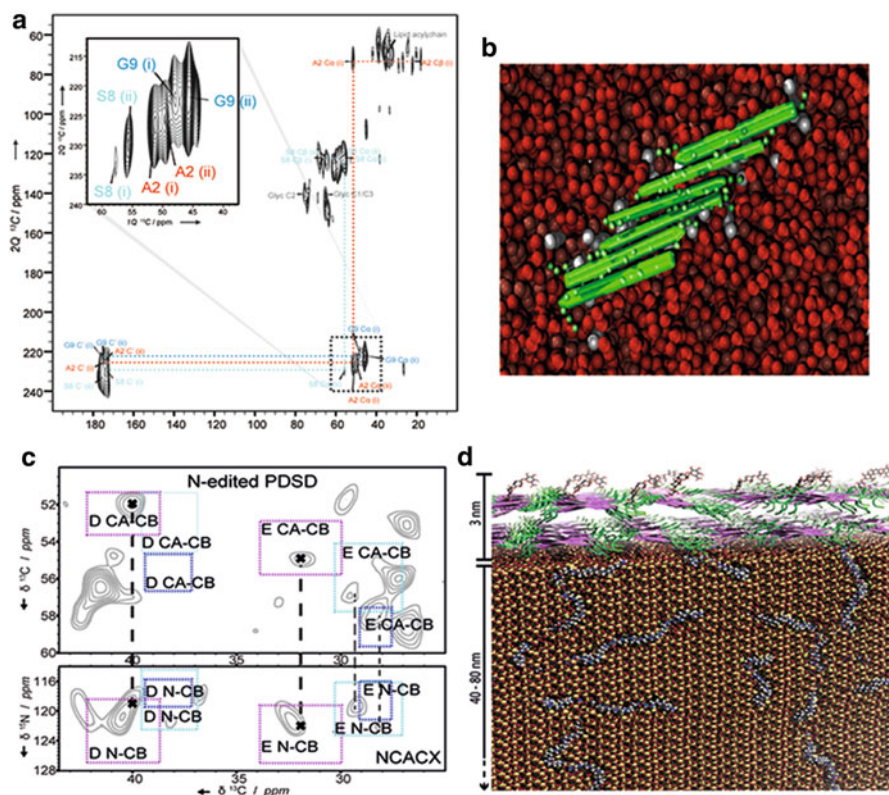


Fig. 4 2D ssNMR data provide unique insight into the molecular structure of complex biomaterials such as liposomal vaccines? (**a**, **b**) and diatom biosilica (**c**, **d**). In the case of (N-terminal, selectively isotope-labeled) $\text{A}\beta$ peptides in different lipid formulations, 2Q/1Q correlation experiments (**a**) provided dihedral angle restraints to model their structural organization in liposomes (**b**, adapted from Ref. [14]). In **c**, results of two-dimensional ^{15}N -edited proton-driven spin-diffusion (PDSD) experiments (*upper panel*) as well as 2D ^{15}N - ^{13}C correlation experiments (such as shown in the *lower panel*) could be used to identify the prevalent types of amino acids as well as their secondary structure fold of diatom biosilica. This information could be used to build, in combination with the DNP results, a model of the supramolecular arrangement of diatom biosilica (**d**, adapted from Ref. [15])

^{15}N CP MAS NMR spectrum. These results can be explained by the assumption that LCPAs are embedded into the silica and thus not accessible for the radicals – in contrast to the peptides. Moreover, the measured DNP signal enhancement factors can be well described by the assumption that the silica-embedded LCPAs are spread over the entire silica phase, whereas the peptides are preferentially found at the surface of the biosilica (see section “[Dynamic Nuclear Polarization \(DNP\)](#)”). Furthermore, based on the considerable signal enhancements provided by DNP solid-state NMR, we were for the first time able to obtain in situ insight into the secondary structure elements of tightly biosilica-associated native proteins in fully [^{13}C , ^{15}N , ^{29}Si]

enriched intact diatom biosilica as is demonstrated in Fig. 4c. Here, results of two-dimensional ^{15}N -edited proton-driven spin-diffusion (PDS) experiments (upper panel) as well as 2D ^{15}N - ^{13}C correlation experiments (such as shown in the lower panel) could be used to identify the prevalent types of amino acids as well as their secondary structure fold. This information could be used to build, in combination with the DNP results, a model of the supramolecular arrangement of diatom biosilica (Fig. 4d).

Drug Delivery Systems

Supramolecular peptide-based carrier systems offer an attractive means to deliver drugs into cells. Weingarth et al. have shown that the integration of solid-state NMR measurements with large- and multi-scale molecular dynamics simulations allows, for the first time, access to the supramolecular structures of a complex peptide-based drug delivery system [34] (Fig. 5). The investigated drug delivery system was assembled from the amphipathic SA2 peptide that is composed of a hydrophobic N-terminal part and a highly negatively charged C-terminus. We first performed ^{13}C - and ^{15}N -detected solid-state measurements with specifically labeled SA2 peptides. Importantly, the solid-state NMR measurements were carried out with a colloidal suspension of specifically labeled peptides, just enough concentrated to form nano-carriers. With the obtained assignments, a beta-strand secondary structure for the hydrophobic peptide part could be readily derived, while the anionic C-terminus could not be detected in dipolar-based experiments. Afterward the secondary structure information was used to perform large-scale coarse-grained simulations, in which we probed the assembly of 2500 SA2 peptides over 54 μs at dilute experimental concentrations (~ 10 mM). These simulations revealed that the peptide assembled to strongly interdigitated and antiparallel beta-sheets, an arrangement that we could validate experimentally with FTIR measurements. Finally, the coarse-grained particles were fine-grained and subjected to a 1 μs long all-atoms simulation, which we validated with several experimental techniques (cryo-EM, AFM, light scattering) and which were very well in agreement with our solid-state

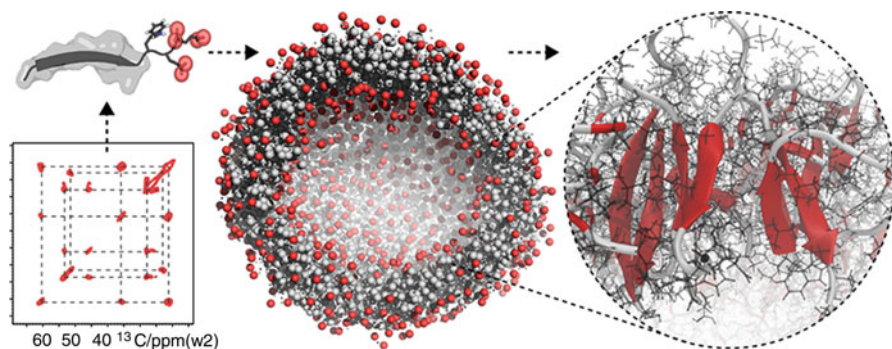


Fig. 5 The integration of solid-state NMR data with large- and multi-scale MD simulations allowed to derive a supramolecular model of a multi-megadalton-sized peptide-based drug delivery system (Adapted from Ref. [34])

NMR data. These simulations also confirmed that the anionic C-termini are very mobile, explaining why they are not visible in dipolar-based NMR experiments.

In cases where the intrinsic viscosity of the sample approaches soluble molecules, isotope labeling is not required to obtain atomic insight into the supramolecular arrangements of biomaterials such as drug delivery systems. An application studied earlier in our laboratory relates to polymeric micelles designed to exhibit a high loading capacity for chemotherapeutic drugs such as paclitaxel or docetaxel [50] that similar to Epo B bind to microtubules (Fig. 3b). In these applications, the combination of low MAS rates (in the order of 1 kHz) and ^1H NOESY (nuclear Overhauser effect) spectroscopy was sufficient to detect aromatic correlations that would be consistent with $\pi - \pi$ stacking among aromatic groups that increase stability and loading capacity of these chemotherapeutic drugs. In cases where the micelle concentrations do not require the use of MAS, ^1H NMR relaxation measurements can be used to infer information about the intrinsic micelle core and more flexible distal segments [51].

Humins

A final demonstration of the use of ssNMR in the context of biomaterials are humins which are by-products formed during the acid-catalyzed dehydration of carbohydrates to bio-based platform molecules, such as hydroxymethylfurfural and levulinic acid. The molecular structure of these humins has not yet been unequivocally established. In collaboration with Weckhuysen et al., we recently [52] applied 2D correlation techniques on ^{13}C -enriched humins. 2D ^{13}C -detected 2Q/1Q spectra and 2D ^1H -detected heteronuclear correlation (HETCOR) were recorded with different excitation schemes. These experiments unambiguously established that the original humins have a furan-rich structure with aliphatic linkers and allowed for a refinement of the molecular structure proposed previously. Solid-state NMR data of alkali-treated ^{13}C -labeled humins showed that an arene-rich structure is formed at the expense of the furanic network during alkaline pretreatment.

Conclusions

The combination of instrumental and methodological improvements including DNP and ^1H -detection under high-speed MAS with state-of-the art structural and computational methods greatly enhances the applicability of ssNMR to complex molecular systems.

In our contribution, we have discussed methodological aspects that can support such studies, and we reviewed applications in the field of protein folding and (mis) assembly as well as in more applied areas of research such as drug delivery or biomass conversion. As we have shown elsewhere [1, 2, 38], the conceptual advancements presented here also offer novel means to study membrane proteins, and they provide increasing possibilities to examine cellular systems. Next to the field of life science, ssNMR plays a leading role in deciphering the molecular details that describe the assembly and workings of complex materials including colloids as

well as inorganic and catalyst materials. Current work in our laboratory suggests that cross-fertilization between the fields of life and material science will further enhance the use of ssNMR in such areas of research.

With the advent of ultrahigh-field NMR systems beyond 1 GHz and the ever-increasing power of computational structural biology as well as advancements in electron microscopy and related fields, further exciting opportunities for ssNMR applications lie ahead of us. Without doubt, ultrahigh-field NMR settings will require tailored as well as novel ssNMR concepts that make efficient use of the increased resolution and sensitivity offered by such instruments. At the same time, further developments in high-field DNP and other hyperpolarization methods will be needed providing a rich field of research for the ssNMR in the future.

Acknowledgments We gratefully acknowledge our collaborators and colleagues for their invaluable contributions to cited publications from our own research group.

These studies were supported through grants from the NWO, the EU, and the NIH, as well as the DFG, the Max Planck Society, and the Volkswagen Foundation.

References

1. Weingarth M, Baldus M. Solid-state NMR-based approaches for supramolecular structure elucidation. *Acc Chem Res.* 2013;46(9):2037–46.
2. Kaplan M, Pinto C, Houben K, Baldus M. Nuclear magnetic resonance (NMR) applied to membrane protein complexes. *Q Rev Biophys.* 2016; 49:e15, <https://doi.org/10.1017/S003358351600010X>.
3. Sattler JJHB, Gonzalez-Jimenez ID, Luo L, Stears BA, Malek A, Barton DG, et al. Platinum-promoted Ga/Al₂O₃ as highly active, selective, and stable catalyst for the dehydrogenation of propane. *Angew Chem.* 2014;126(35):9405–10. Wiley-VCH Verlag.
4. van der Stam W, Gradmann S, Altantzis T, Ke X, Baldus M, Bals S, et al. Shape control of colloidal Cu₂-xS polyhedral nanocrystals by tuning the nucleation rates. *Chem Mater.* American Chemical Society; 2016;28(18):6705–6715.
5. Renault M, Tommassen-van Boxtel R, Bos MP, Post JA, Tommassen J, Baldus M. Cellular solid-state nuclear magnetic resonance spectroscopy. *Proc Natl Acad Sci.* 2012;109(13):4863–8.
6. Renault M, Pawsey S, Bos MP, Koers EJ, Nand D, Tommassen-van Boxtel R, et al. Solid-state NMR spectroscopy on cellular preparations enhanced by dynamic nuclear polarization. *Angew Chem Int Ed.* 2012;51(12):2998–3001. Wiley-VCH Verlag. Available from <http://doi.wiley.com/10.1002/anie.201105984>.
7. Baker LA, Daniëls M, van der Cruijnsen EAW, Folkers GE, Baldus M. Efficient cellular solid-state NMR of membrane proteins by targeted protein labeling. *J Biomol NMR.* 2015;62(2):199–208.
8. Labokha AA, Gradmann S, Frey S, Hülsmann BB, Urlaub H, Baldus M, et al. Systematic analysis of barrier-forming FG hydrogels from *Xenopus* nuclear pore complexes. *EMBO J.* 2012;32(2):204–18.
9. Kaplan M, Narasimhan S, de Heus C, Mance D, Van Doorn S, Houben K, et al. EGFR dynamics change during activation in native membranes as revealed by NMR. *Cell.* 2016;167(5):1241–1251.e11. <https://doi.org/10.1016/j.cell.2016.10.038>.
10. Barbieri L, Bertini I, Luchinat E, Secci E, Zhao Y, Banci L, et al. Atomic-resolution monitoring of protein maturation in live human cells by nMr. *Nat Chem Biol.* 2013;9(5):297–9.
11. Ni QZ, Daviso E, Can TV, Markhasin E, Jawla SK, Swager TM, et al. High frequency dynamic nuclear polarization. *Acc Chem Res.* 2013;46(9):1933–41.

12. Koers EJ, van der Crujisen EAW, Rosay M, Weingarth M, Prokofyev A, Sauvee C, et al. NMR-based structural biology enhanced by dynamic nuclear polarization at high magnetic field. *J Biomol NMR*. 2014;60(2–3):157–68.
13. Kaplan M, Cukkemane A, van Zundert GCP, Narasimhan S, Daniëls M, Mance D, et al. Probing a cell-embedded megadalton protein complex by DNP-supported solid-state NMR. *Nat Methods*. 2015;12(7):649–52.
14. Koers EJ, López-Deber MP, Weingarth M, Nand D, Hickman DT, Mlaki Ndao D, et al. Dynamic nuclear polarization NMR spectroscopy: revealing multiple conformations in lipid-anchored peptide vaccines. *Angew Chem Int Ed*. 2013;52(41):10905–8.
15. Jantschke A, Koers E, Mance D, Weingarth M, Brunner E, Baldus M. Insight into the supramolecular architecture of intact diatom biosilica from DNP-supported solid-state NMR spectroscopy. *Angew Chem Int Ed*. 2015;54(50):15069–73.
16. Mance D, Gast P, Huber M, Baldus M, Ivanov KL. The magnetic field dependence of cross-effect dynamic nuclear polarization under magic angle spinning. *J Chem Phys*. 2015;142(23):234201.
17. Sauvee C, Rosay M, Casano G, Aussenac F, Weber RT, Ouari O, et al. Highly efficient, water-soluble polarizing agents for dynamic nuclear polarization at high frequency. *Angew Chem Int Ed*. 2013;52(41):10858–61.
18. van der Crujisen EAW, Koers EJ, Sauvee C, Hulse RE, Weingarth M, Ouari O, et al. Biomolecular DNP-supported NMR spectroscopy using site-directed spin labeling. *Chem Eur J*. 2015;21(37):12971–7.
19. Perras FA, Reinig RR, Slowing II, Sadow AD, Pruski M. Effects of biradical deuteration on the performance of DNP: towards better performing polarizing agents. *Phys Chem Chem Phys*. 2016;18(1):65–9. The Royal Society of Chemistry.
20. Mathies G, Caporini MA, Michaelis VK, Liu Y, Hu K-N, Mance D, et al. Efficient dynamic nuclear polarization at 800 MHz/527 GHz with trityl-nitroxide biradicals. *Angew Chem Int Ed*. 2015;54(40):11770–4.
21. Heise H, Luca S, de Groot BL, Grubmüller H, Baldus M. Probing conformational disorder in neurotensin by two-dimensional solid-state NMR and comparison to molecular dynamics simulations. *Biophys J*. 2005;89(3):2113–20.
22. Fricke P, Mance D, Chevelkov V, Giller K, Becker S, Baldus M, et al. High resolution observed in 800 MHz DNP spectra of extremely rigid type III secretion needles. *J Biomol NMR*. 2016;65:121–6.
23. Chevelkov V, Rehbein K, Diehl A, Reif B. Ultrahigh resolution in proton solid-state NMR spectroscopy at high levels of deuteration. *Angew Chem Int Ed*. 2006;45(23):3878–81.
24. Dannatt HRW, Felletti M, Jehle S, Wang Y, Emsley L, Dixon NE, et al. Weak and transient protein interactions determined by solid-state NMR. *Angew Chem*. 2016;128(23):6750–3.
25. Linser R, Dasari M, Hiller M, Higman V, Fink U, Lopez del Amo J-M, et al. Proton-detected solid-state NMR spectroscopy of fibrillar and membrane proteins. *Angew Chem Int Ed*. 2011;50(19):4508–12.
26. Ward ME, Shi L, Lake E, Krishnamurthy S, Hutchins H, Brown LS, et al. Proton-detected solid-state NMR reveals intramembrane polar networks in a seven-helical transmembrane protein proteorhodopsin. *J Am Chem Soc*. 2011;133(43):17434–43.
27. Sinnige T, Daniëls M, Baldus M, Weingarth M. Proton clouds to measure long-range contacts between nonexchangeable side chain protons in solid-state NMR. *J Am Chem Soc*. 2014;136(12):4452–5.
28. Mance D, Sinnige T, Kaplan M, Narasimhan S, Daniëls M, Houben K, et al. An efficient labelling approach to harness backbone and side-chain protons in ^1H -detected solid-state NMR spectroscopy. *Angew Chem*. 2015;127(52):16025–9.
29. Medeiros-Silva J, Mance D, Daniels M, Houben K, Baldus M, et al. ^1H -detected solid-state NMR studies of water-inaccessible proteins in vitro and in situ. *Angew Chem Int Ed Engl*. 2016;55(43):13606–13610.

30. Weingarth M, van der Crujisen EAW, Ostmeyer J, Lievestro S, Roux B, Baldus M. Quantitative analysis of the water occupancy around the selectivity filter of a K⁺ channel in different gating modes. *J Am Chem Soc.* 2014;136(5):2000–7.
31. Andreas LB, Jaudzems K, Stanek J, Lalli D, Bertarello A, Le Marchand T, et al. Structure of fully protonated proteins by proton-detected magic-angle spinning NMR. *Proc Natl Acad Sci U S A.* 2016;113(33):9187–92.
32. Weingarth M, Ader C, Melquiond ASJ, Nand D, Pongs O, Becker S, et al. Supramolecular structure of membrane-associated polypeptides by combining solid-state NMR and molecular dynamics simulations. *Biophys J.* 2012;103(1):29–37.
33. Marrink SJ, Risselada HJ, Yefimov S, Tieleman DP, de Vries AH. The MARTINI force field: coarse grained model for biomolecular simulations. *J Phys Chem B.* 2007;111(27):7812–24. American Chemical Society.
34. Rad-Malekshahi M, Visscher KM, Rodrigues JPGLM, de Vries R, Hennink WE, Baldus M, et al. The supramolecular organization of a peptide-based nanocarrier at high molecular detail. *Am Chem Soc.* 2015;137(24):7775–84. American Chemical Society.
35. Weingarth M, Prokofyev A, van der Crujisen EAW, Nand D, Bonvin AMJJ, Pongs O, et al. Structural determinants of specific lipid binding to potassium channels. *J Am Chem Soc.* 2013;135(10):3983–8.
36. van der Crujisen EAW, Nand D, Weingarth M, Prokofyev A, Hornig S, Cukkemane AA, et al. Importance of lipid–pore loop interface for potassium channel structure and function. *Proc Natl Acad Sci.* 2013;110(32):13008–13.
37. Gradmann S, Ader C, Heinrich I, Nand D, Dittmann M, Cukkemane A, et al. Rapid prediction of multi-dimensional NMR data sets. *J Biomol NMR.* 2012;54(4):377–87.
38. Baker LA, Baldus M. Characterization of membrane protein function by solid-state NMR spectroscopy. *Curr Opin Struct Biol.* 2014;27:48–55.
39. Tycko R. Solid-State NMR. Studies of amyloid fibril structure. *Annu Rev Phys Chem.* 2011;62(1):279–99.
40. Heise H, Hoyer W, Becker S, Andronesi OC, Riedel D, Baldus M. Molecular-level secondary structure, polymorphism, and dynamics of full-length {alpha}-synuclein fibrils studied by solid-state NMR. *Proc Natl Acad Sci U S A.* 2005;102(44):15871–6.
41. Andronesi OC, von Bergen M, Biernat J, Seidel K, Griesinger C, Mandelkow E, et al. Characterization of Alzheimer's-like paired helical filaments from the core domain of tau protein using solid-state NMR spectroscopy. *J Am Chem Soc.* 2008;130(18):5922–8.
42. Daebel V, Chinnathambi S, Biernat J, Schwalbe M, Habenstein B, Loquet A, et al. β -sheet core of tau paired helical filaments revealed by solid-state NMR. *J Am Chem Soc.* 2012;134(34):13982–9.
43. Schneider R, Schumacher MC, Mueller H, Nand D, Klaukien V, Heise H, et al. Structural characterization of polyglutamine fibrils by solid-state NMR spectroscopy. *J Mol Biol.* 2011;412(1):121–36.
44. Kim H-Y, Heise H, Fernandez CO, Baldus M, Zweckstetter M. Correlation of amyloid fibril beta-structure with the unfolded state of alpha-synuclein. *Chembiochem.* 2007;8(14):1671–4.
45. Poyraz O, Schmidt H, Seidel K, Delissen F, Ader C, Tenenboim H, et al. Protein refolding is required for assembly of the type three secretion needle. *Nat Struct Mol Biol.* 2010;17(7):788–92.
46. Kumar A, Heise H, Blommers MJJ, Krastel P, Schmitt E, Petersen F, et al. Interaction of epothilone B (Patupilone) with microtubules as detected by two-dimensional solid-state NMR spectroscopy. *Angew Chem Int Ed.* 2010;49(41):7504–7.
47. Yan S, Guo C, Hou G, Zhang H, Lu X, Williams JC, et al. Atomic-resolution structure of the CAP-Gly domain of dynactin on polymeric microtubules determined by magic angle spinning NMR spectroscopy. *Proc Natl Acad Sci U S A.* 2015;112(47):14611–6.
48. Courchaine EM, Lu A, Neugebauer KM. Droplet organelles? *EMBO J.* 2016;35(15):1603–1612.

49. Ader C, Frey S, Maas W, Schmidt HB, Goerlich D, Baldus M. Amyloid-like interactions within nucleoporin FG hydrogels. *Proc Natl Acad Sci.* 2010;107(14):6281–5.
50. Shi Y, van Steenberg MJ, Teunissen EA, Novo L, Gradmann S, Baldus M, et al. Π – Π stacking increases the stability and loading capacity of thermosensitive polymeric micelles for chemotherapeutic drugs. *Biomacromolecules.* 2013;14(6):1826–37. American Chemical Society.
51. de Graaf AJ, Boere KWM, Kemmink J, Fokkink RG, van Nostrum CF, Rijkers DTS, et al. Looped structure of flowerlike micelles revealed by ^1H NMR relaxometry and light scattering. *Langmuir.* 2011;27(16):9843–8.
52. van Zandvoort I, Koers EJ, Weingarh M, Bruijninx PCA, Baldus M, Weckhuysen BM. Structural characterization of ^{13}C -enriched humins and alkali-treated ^{13}C humins by 2D solid-state NMR. *Green Chem.* 2015;17(8):4383–92.